

ON THE THERMAL DEFORMATION ANALYSES OF CVD SILICON-CARBIDE MIRROR

M. C. Lin and K. L. Tsang

Synchrotron Radiation Research Center, Hsinchu 300, Taiwan

Abstract

Due to the high thermal conductivity and low expansion coefficient, the CVD silicon-carbide mirrors have been chosen as the high thermal loaded optical components for the undulator beamlines at SRRC. The deformations of these mirrors exposed to the highly localized undulator photon beams have been studied. The commercially available analytical codes, ANSYS and MSC/PATRAN, have been employed for the 3-D model analysis. The temperature distribution and hence the deformation of the thermally loaded mirror surfaces have been studied. The analytical results show that the deformation is not symmetric even though the thermal loading is symmetric. This is caused by the clamping method of the mirror or its holder. The effect of the asymmetric deformation will be also discussed.

1 INTRODUCTION

The thermal effect on the beamline optical devices exposed to a strong photon beam such as the undulator radiation source has been studied. Nian and his colleagues[1] at APS studied the surface temperature and thermal stress on a Glidcop fixed mask of the front end of an insertion device beamline. With a maximum power density of 519 W/mm², it was shown that a miss steered x-ray beam would cause a maximum effective stress of 320 Mpa on the mask. Senf and his colleagues[2] calculated the thermal effect on the entrance slit of a spherical grating monochromator (SGM) for an undulator beamline at BESSY. They showed that the Glidcop slit blade would expand about 16 μm with a thermal loading of 50 W and a maximum power density of 780 W/mm².

In this study, we investigate the temperature distribution and deformation on the surface of a plane grating used for an undulator beamline. This grating will be exposed to a thermal power of 20 W and the peak power density is about 0.16 W/mm². Since this grating will be used in a high performance beamline, an effective cooling of this grating is required. Because of the high thermal conductivity, k 0.330 W/mm°C, low expansion coefficient, α 2.2 PPM/°C, and the excellent distortion figure of merit, $k/\alpha = 150$ μm/W, CVD silicon carbide (SiC) is chosen for the grating's substrate. However, an internal cooling method is difficult to manufacture in the CVD SiC block. We are searching for an easy and effective enough cooling mechanism for this optics. Fig. 1 shows the holding and cooling mechanism of the

grating block of only one half of the full length. The grating block is sandwiched by two copper plates which are connected to the water-cooled copper block. Copper has thermal conductivity k 0.401 W/mm°C, expansion coefficient α 16.6 PPM/°C, and the distortion figure of merit, k/α 24.2 μm/W. The grating is 120 mm long, 21 mm wide, and 25 mm high. The cooling block has two water channels with diameter of 4 mm. The incoming water is kept at 25 °C and is flowing serially. We will use the finite element analyses to study the temperature distribution and the thermal deformation of the grating surface.

2 FINITE ELEMENT MODEL

As shown in Fig. 1, the origin (0,0,0) of the (X,Y,Z) coordinates is set at the center of the grating's surface. The grating block is held by three points at (10.5, -25, 0), (-10.5, -25, -25), and (-10.5, -25, 25). In the 3D finite element analyses, the commercially available analytical code ANSYS[3] was adopted as the solver, while another code MSC/PATRAN[4] was used as pre- and post-processors for easy modeling and result presenting. Because of the symmetries of the grating block and the heating pattern, only one half of the block has to be modeled. The 20-node hexahedral element is the only element adopted in this model. Totally there are 2612

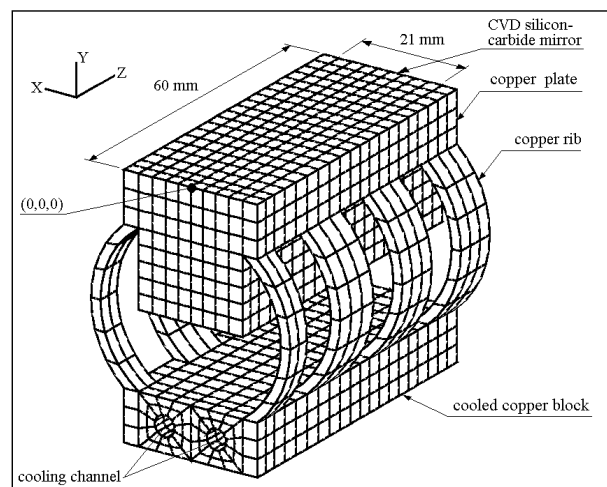


Fig.1 The holding and cooling mechanism of the grating block of only one half of the grating. The finite element mesh is also shown.

elements and 13864 nodes. The finite element mesh is

also shown in Fig. 1.

With the total absorbed thermal power of 20 W and the characteristics of the undulator beam which gives the beam foot-print of 50 mm × 10 mm, the thermal power distribution $P(X,Z)$ can be simulated by a bivariate normal distribution[5]:

$$P(X,Z) = \frac{P_{total}}{2\pi\sigma_X\sigma_Z} \exp\left(-\frac{\left(\frac{X}{\sigma_X}\right)^2 + \left(\frac{Z}{\sigma_Z}\right)^2}{2}\right) \quad (1)$$

in which P_{total} is the total power absorbed on the grating surface, σ_X and σ_Z the standard deviation of X and Z. In this case, P_{total} is 20 W, σ_X and σ_Z are chosen as 2 mm and 10 mm, respectively. It can be obtained that the maximum power density is 0.159 W/mm². The power distribution is shown in Fig. 2 as a function of Z for several X values.

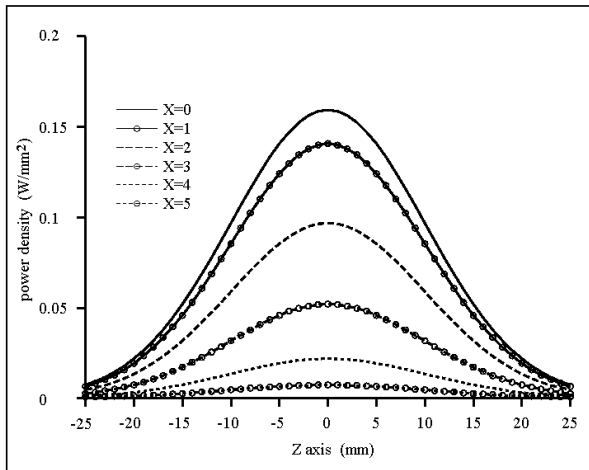


Fig. 2 Bivariate normal power distribution of total 20 W power along Z-axis at various X location.

With assumptions of uniform surface heat flux on the wall of cooling channel and fully developed laminar cooling water flow, the surface convection heat transfer coefficient h is found to be[6]

$$h = 4.36\left(\frac{k_w}{D}\right) \quad (2)$$

in which k_w is the conduction coefficient of water, D the diameter of the circular cooling channel. For the case described above, we obtain $h = 668.7 \times 10^{-6}$ W/mm² °C. With the laminar flow condition, the water flow in the cooling channels must have an average velocity less than 0.49 m/sec. Assuming the average water velocity is 0.4 m/sec, which is equivalent to a flow rate of 0.3 liter/min, and the incoming water is kept at 25 °C, it is found that

the temperature of the cooling water is raised by 0.95 °C.

3 RESULTS AND DISCUSSIONS

Fig. 3 shows the equilibrium temperature distribution on the surface at different locations along either the X-direction or the Z-direction. The maximum temperature rise is 19.4 °C and locates at the central point. Clearly, the temperature distribution is maintained at a similar shape of the original power density, but with much less difference in magnitude. The maximum temperature difference across the whole surface is less than 3 °C. The temperatures at the locations at $Z > 25$ mm in the X-direction are same. This is due to the fact that the grating is much longer than the foot-print of the photon beam. In the area near the center, the temperature changes more rapidly in the X-direction than that in the Z-direction.

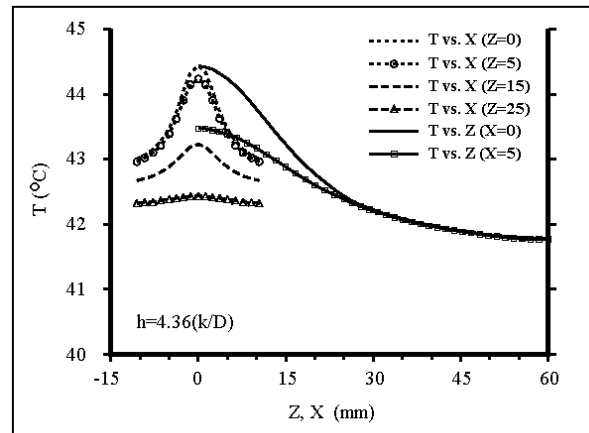


Fig.3 The equilibrium temperature distribution on the mirror surface after exposed to a thermal power of 20 W, where Z is from 0 to 60 mm and X from -11 to 11 mm.

The quality of the mirror's surface shape will greatly affect the mirror's performance. Therefore, how well the mirror's surface shape is maintained after exposed to the thermal loading becomes very important. We can use the temperature distribution and the mirror's holding method to calculate the surface deformation. As far as the mirror's performance concerned, the change of the shape in the Y-direction is important. The change of the surface's height in Y-direction is shown in Fig. 4. Overall the change of the surface's height is small. As observed, the maximum U_y is 1.29 μm. Furthermore, the change of the surface's height is similar to the temperature distribution with some differences in the Z-direction, but is very different from the temperature distribution in the X-direction. These differences are caused by the holding mechanism. This effect is seen more clearly in Fig. 5, in which the tilt of the surface is shown. Obviously, the surface's deformation is less severe in the Z-direction than

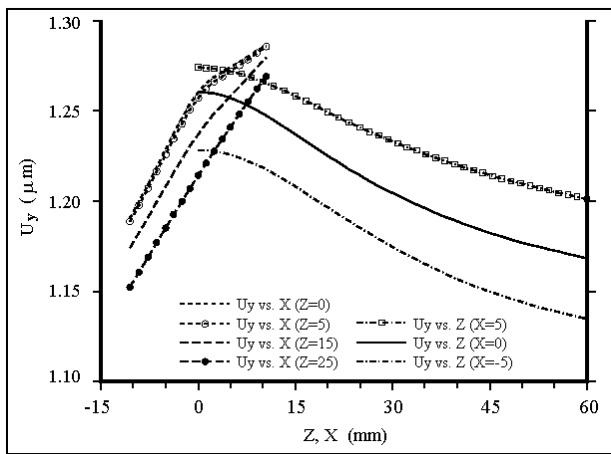


Fig. 4 Variation of the mirror surface's height in the Y-direction, where Z is form 0 to 60 mm and X from -11 to 11 mm.

in the X-direction. The surface is not only deformed locally but also is tilted, as shown in the curves of $\Delta U_y / \Delta X$. The tilt of the surface can be easily seen in the curves of $\Delta U_y / \Delta X$ at $Z > 30$ mm. A tilt of $6.7 \mu\text{rad}$ is obtained even there is no temperature difference. The tilt of the surface is caused by the holding mechanism.

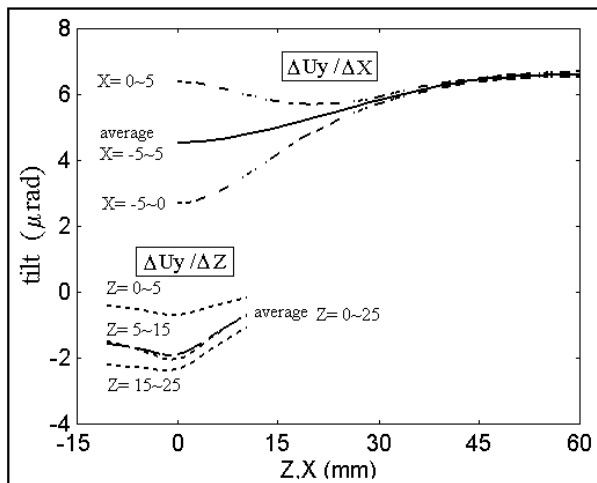


Fig. 5 Mirror surface tilt along both X- and Z-axes after the mirror has exposed to a thermal power of 20 W, where Z is form 0 to 60 mm and X from -11 to 11 mm.

4. CONCLUSIONS

With the help of the finite element analysis, we have studied the temperature distribution and the surface deformation of a CVD SiC mirror when the mirror is exposed to an undulator beam of 20 W. A simple mirror holding mechanism and an easy cooling method have been used for the study. If the mirror is held by three-points as described in the text, and an easy in-direct cooling system is used, then several simulation results

have been obtained, as shown below.

1. The temperature distribution on the surface is pretty uniform with a maximum temperature difference of less than 3°C . However, the temperature distribution is still showing a shape similar to that of the power loading.
2. The change of the surface height in the Y-direction, where the change will degrade the performance greatly, is very different from the temperature change. The surface is not only deformed locally, due to the temperature difference, but also tilted. The tilt is caused by the holding mechanism.
3. A tilt of greater than $6 \mu\text{rad}$ can be obtained from a non-proper holding mechanism.

Further studies on the effects of mirror holding mechanism as well as the cooling method are on the way. As far as this application is concerned, it seems that a surface deformation of less than $2 \mu\text{rad}$ is reachable even a simple side-cooling method is used.

REFERENCES

- [1] F. Senf, U. Menthel, and W.B. Peatman, "Heat Load Problem of an Entrance Slit on an Undulator Beamline," *Rev. Sci. Instrum.*, Vol. 66, pp. 2224-2227, 1995
- [2] H.L. Thomas Nian, D. Shu, I.C. Albert Sheng, and T.M. Kuzay, "Thermo-mechanical Analysis of Fixed Mask 1 for the Advanced Photon Source Insertion Device Front Ends," *Nuclear Instruments and Methods in Physics Research A*, Vol. 347, pp. 657-663, 1994
- [3] Program ANSYS, a product of Swanson Analysis System, Inc. is a commercial available 3D finite element code.
- [4] MSC/PATRAN, a product of MacNeal-Schwendler Corporation (MSC), is a commercial available 3D code that can be used as per-processor and post-processor for some other finite element analysis codes.
- [5] Jay L. Devore, "Probability and Statistics for Engineering and the Sciences," Second Edition, Chap. 12, 1987
- [6] F. P. Incropera and D. P. Witt, "Fundamentals of Heat and Mass Transfer," Second Edition, Chap. 8, 1985